Turkish Journal of Civil Engineering, 2024 xxxx-xxxx, Paper xxx, ***Research Article***

Design and Tests of Structural Post-Tensioned Glass T-Beams

Emrullah KOCA[1*]
Ahmet TÜRER[2]

ABSTRACT

Glass manifests superior properties with high strength and transparency although it may not be considered as a commonly used structural material. This study targets to improve the structural performance of glass by post-tensioning; a series of T-shaped glass beams are tested to develop a proper and safe design. Traditionally, glass is widely used in buildings as windows where its brittleness and strength capacity are not significant. Architects prefer to use glass in the structural field because of aesthetics, recyclability, and transparency. Although there is more demand for the usage of glass as a structural material, a common fear of its brittle nature and lack of research about its structural behavior have mostly hindered it. Since glass is a brittle material and has high compressive strength in the order of 400 to 800 MPa and lower tensile strength (40 to 120 MPa), post-tensioning to target distributed loads is investigated to increase its fracture capacity and even obtain a post-cracking ductile behavior. In this study, several material tests are conducted to confirm the theoretical mechanical properties of glass. After obtaining the bending and compressive strength of the glass, Finite Element Models (FEMs) of the T-beams were generated and analytical hand calculations were conducted. The tests of T-shaped annealed (float) and tempered (toughened) glass beams with and without post-tensioning were conducted. The results of the experiments were compared with the analytical hand calculations and FEM results. A favorable outcome of this study is that float glass' post cracking strength has been drastically increased and a ductile post-cracking performance is obtained. Tempered glass has a brittle response but with much higher strength, with about 4 times the capacity of annealed glass T-beams

Keywords: Post-tensioned glass beam, T-beam, structural glass, glass beam test.

Note:
- This paper was received on December 14, 2023 and accepted for publication by the Editorial Board on April 5, 2024.
- Discussions on this paper will be accepted by xxxxxxx xx, xxxx.

• https://doi.org/10.18400/tjce.1405084

1 Middle East Technical University, Department of Civil Engineering, Ankara, Türkiye
koca.emrullah@metu.edu.tr - https://orcid.org/0000-0002-0459-7946

2 Middle East Technical University, Department of Civil Engineering, Ankara, Türkiye
aturer@metu.edu.tr - https://orcid.org/0000-0002-2214-1387

* Corresponding author

1. INTRODUCTION

Glass is an inorganic, visco-elastic, and isotropic material with a non-crystalline molecular structure. The typical composition of glass consists of silica-SiO2 (70-74%), lime-CaO (5-12%), soda-Na_2O (12-16%), and other chemical elements with influence on transmittance, thermal properties, tensile strength, fracture toughness, and color, etc. Considered a structural material, no plastic deformation occurs before the failure and it breaks suddenly similar to high-strength concrete. There are several types of glass such as float (annealed), heat-strengthened, fully tempered, laminated, and insulated. Typical fractures of different glass types are demonstrated in Fig. 1.

Fig. 1 - Typical fracture shapes of glass types [1]

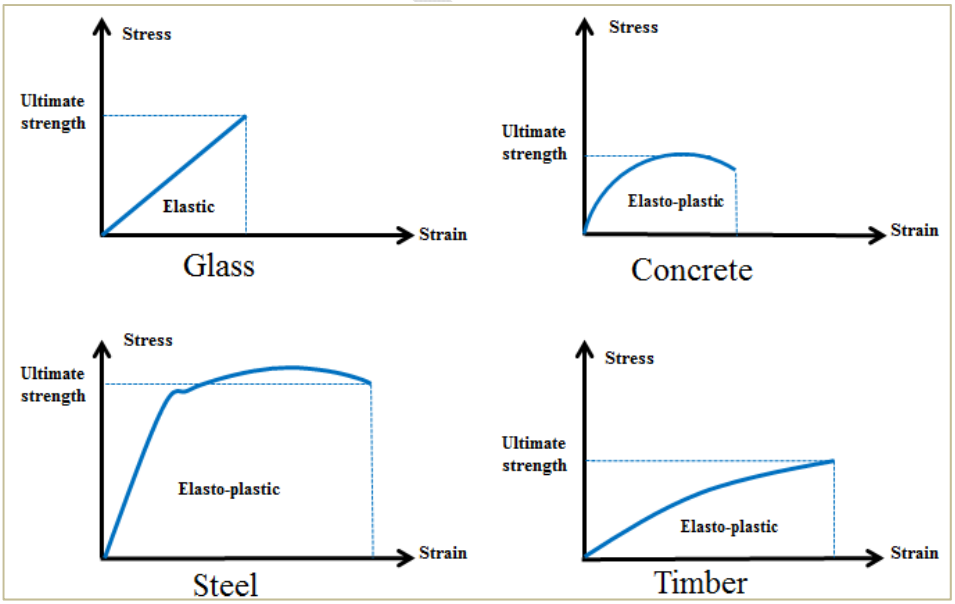

Fig. 2 - Typical stress-strain graphs of structural materials under bending

The compressive strength of glass is about ten times larger than its tensile strength, so the breakage of a glass beam is mostly governed by its tensile strength. Therefore, reinforced glass beams using rebars or even with post-tensioning would cause significant strength and ductility increase making it useable as a structural material such as in the case of reinforced concrete. Additional advantages such as prefabrication, visually pleasing, and high strength make glass superior to concrete under certain applications. Some mechanical and physical properties of glass are as follows: density (ρ)=2500 kg/m^3, modulus of elasticity (E)=70 GPa, shear modulus (G)=30 GPa, and Poisson's ratio (ν)=0.23 [2, 3]. Typical stress-strain curves of structural materials such as glass, concrete, steel, and timber are compared in Fig. 2.

It should be noted that the graphs are not to scale. It can be inferred from the graphs that glass has brittle behavior somewhat like high-strength concrete and timber.

This research explores using a technique well-established in concrete construction (post-tensioning) for a new material (glass). The study investigates how the T-shaped cross-section, which is efficient for carrying loads, can be combined with post-tensioning for glass beams. The research includes data for two commonly used types of architectural glass, providing a broader understanding of the technique's effectiveness.

1.1. Post-Tensioning Application

Pre-stressing can be applied to members in two ways, pre-tensioning or post-tensioning. In pre-tensioned members, the pre-stressing strands are tensioned against restraining before the material is cast and the strands are released after hardening. Post-tensioning involves installing and stressing strand or bar tendons after the material has been placed, hardened, and attained a minimum compressive strength for the transfer. The function of post-tensioning is to generate a compression field, especially in regions where tensile stresses develop. Post-tensioning below the neutral axis in a simply supported beam would generate compression at the bottom and create an upward deflection; in this way, minimizes tensile stresses and beam deflections under loading in the gravitational direction. The post-tensioning wire may be placed with different geometric layouts to optimize the negative bending and camber to suit loading patterns. In this study, galvanized steel wire rope with an 8 mm diameter and ultimate strength (f_u) of 750 MPa was used as a post-tensioning member.

The advantages of using glass beams with post-tensioning can be considered as a) an increase in cracking capacity, b) ductility gained by post-cracking strength, c) no losses because of shrinkage (as in the case of post-tensioned concrete), d) making use of high strength of glass which is about 400 to 800 MPa in compression and about 40 MPa in tension, and e) appealing view of the transparent glass material.

1.2. Literature Review

The concept of post-tensioned glass beams has currently been studied in a limited number of research papers. The main goals of post-tensioning structural glass beams were explained as increasing the initial fracture strength of the glass and providing a significant post-fracture residual load-carrying capacity. However, in all of the studies, post-tensioning was applied in different ways and geometries.

Cupac *et al.* [4] offer a valuable starting point for anyone interested in understanding the potential and current advancements in post-tensioned glass beam technology. It provides a comprehensive survey of the field, highlighting the benefits, design considerations, and ongoing research directions for this promising structural application.

Belis *et al.* [5] studied the enhancement of the buckling strength of glass beams using lateral restraints focusing on load-bearing glass beams, subjected to different loading types. They concluded that the addition of point-wise lateral restraints has a very important positive effect on the load-bearing capacity of a beam subjected to a concentrated load.

Louter *et al*. [6] investigated the post-tensioning load transfer mechanism from the cable to the glass beam at its ends. In this research, it was observed that the most essential aspect of post-tensioning glass beams seems to be the alignment of the end pieces to match the inclination of post-tensioning forces.

Belis, Louter, *et al.* [7] worked on the effect of post-tensioning on the buckling behavior of a T- shaped glass beam. The conclusion was that the geometry of the prototype had relatively good resistance to buckling and the beam failed due to the fracture of glass.

Louter [8] studied the aspects of embedded reinforcement in layered glass beams numerically and experimentally. It was concluded that both the numerical and the numerical models provide a promising method for describing the structural response of reinforced glass beams.

Louter *et al.* [9] conducted experimental tests on beams with mechanically anchored post-tensioning tendons integrated at the top and bottom edges of the glass beams. It was concluded that post-tensioning using mechanically anchored or adhesively bonded tendons was a feasible concept, which provided increased initial fracture strength and enhanced post-fracture performance.

Engelmann and Weller [10] studied the results of three 9 m glass beams post-tensioned with 24 mm high-grade spiral cables. The primary aim was to describe the load-bearing behavior of large-span, post-tensioned glass beams and to determine their ultimate load-bearing capacity. The secondary aim was to present a practical application by designing a 9 m pedestrian bridge. It was concluded that numerical methods were suitable for preliminary design. Furthermore, a 9 m span is said to be feasible and confirmed with test results.

Cupac *et al.* [11] investigated the mechanisms that can cause failure in post-tensioned glass beams. Their design used a flat stainless-steel tendon bonded with adhesive to the underside of the glass. The potential failure modes included the tendon snapping, the glass itself fracturing under tension, and the adhesive bond failing at the point where the load is introduced. The researchers compared the results of their physical model with a computer simulation, finding good agreement between the two. Finally, they used this validated model to conduct a parametric study, which explored how different beam design choices affect the effectiveness of post-tensioning in glass beams.

Several other studies have been found in the literature, reporting the behavior of laminated glass beams with or without post-tensioning [12-16]. The lamination process allows the usage of multiple layers of glass and post-cracking behavior is better controlled preventing shattering.

Although post-tensioning was applied in different patterns and shapes, more research should be done about structural glass to effectively use it as a structural material. This study aims to

investigate numerical and experimental aspects of glass T beams with and without post-tensioning on float and tempered glass.

2. MATERIAL TESTS

Several compression and bending (indirect tension) material tests were conducted to confirm the theoretical mechanical properties of glass. Compression tests were conducted with cubes of float glass in 60x60x60 mm dimensions. However, the cubes were prepared using 10 layers of 60x60x6 mm thick glass pieces piled on top of each other. The tests (Fig. 3) yielded a compressive strength of 267 MPa, which is much lower than the theoretical 400 MPa. Specimens had partial cracking and portion spalling, which indicated an uneven stress distribution. The layered characteristic of test specimens is deemed to cause small gaps and variations in stress; therefore, the compressive strength was assumed as 400 MPa for post-tensioned T beam tests, and no compression failure was observed. Although the shear capacity of glass is not broadly referenced, the compressive and tensile capacities were utilized together with the Coulomb-Mohr Fracture Criterion [14] to calculate shear strength as 36.4 MPa for float glass and 92.3 MPa for tempered glass.

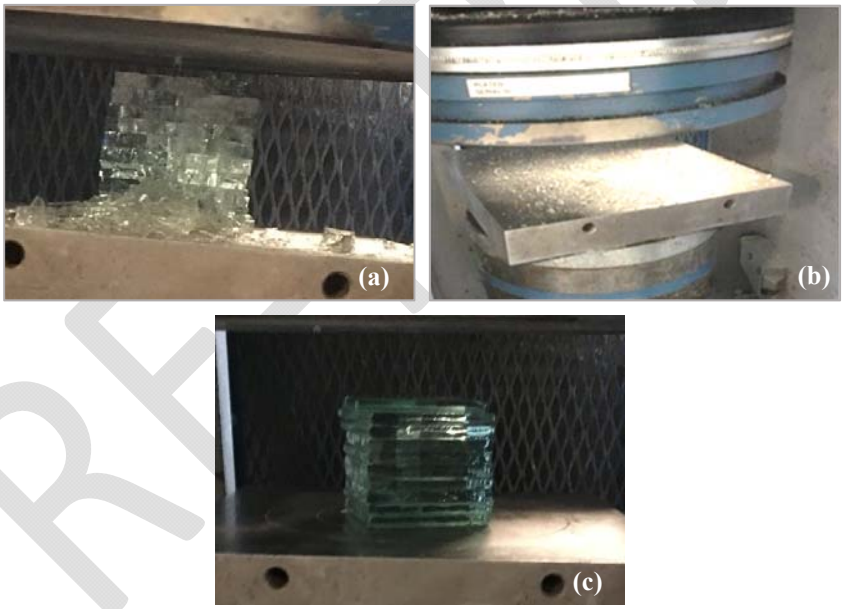

Fig. 3 - A glass cube a) before, b) exploded after, and c) premature failure after the compression test

Float and tempered glass samples were also tested under bending both in their weak and strong axes to determine the bending (indirect tension) strength of glass. The reason for testing samples both in their weak and strong axes was to see how the characteristic strength changes concerning the glass edge placement. Three samples from each 1000x100x6mm and 1000x200x6 mm dimensioned specimens were loaded from two 1/3 length points until they

were fractured (Fig. 4). The same bending test procedure was conducted on three sets of samples. Load-displacement graphs were obtained by post-processing data recorded from the data logger. The load-displacement graphs of float glass specimens placed in their weak axes are given in Fig. 5(a), and their strong axes are shown in. Fig. 5(b).

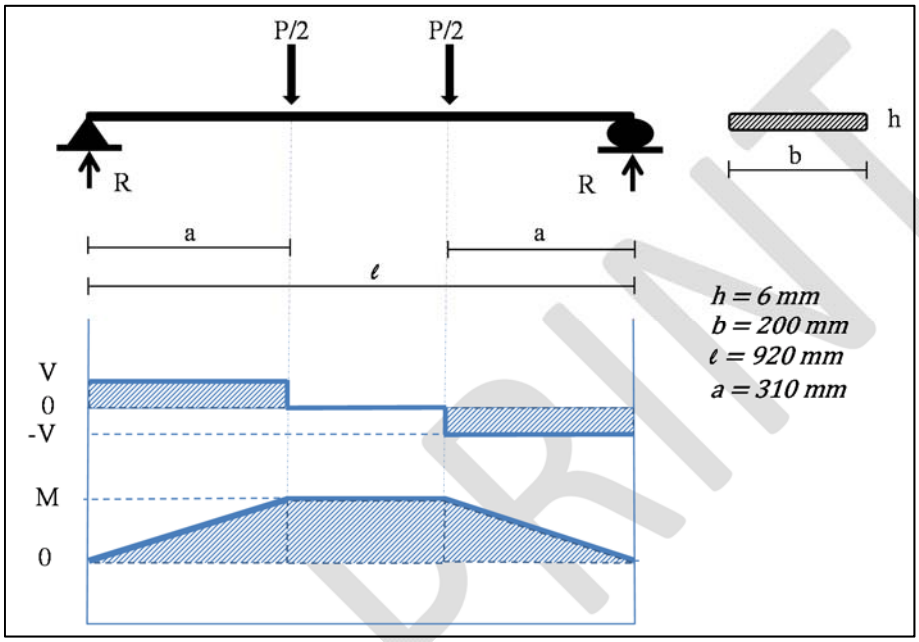

Fig. 4 - Test setup and shear & moment diagrams of the test specimens

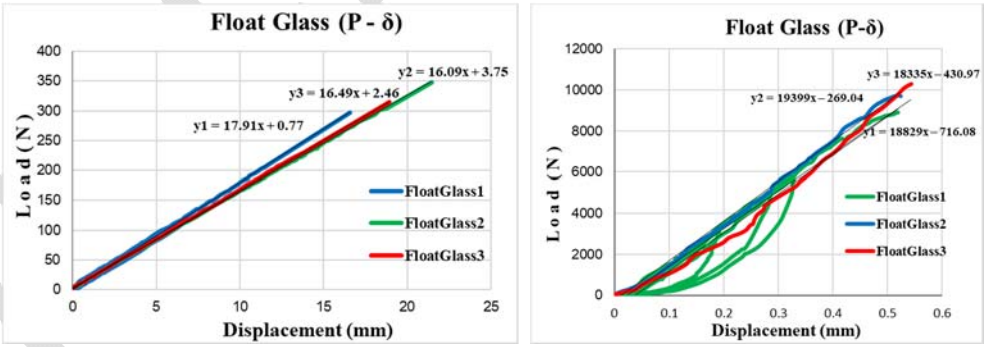

(a) (b)

Fig. 5 - Bending test load-displacement graph of float glass (a) weak axis and (b) strong axis

Bending strength (σ) (indirect tension) and elastic modulus (E) were calculated using standard engineering formulas and listed in Table 1 together with their theoretical counterparts. The mean bending strength and elastic modulus were comparable to the values found in the literature. The characteristic bending strength and modulus of elasticity (with a %5 probability of lowering) were obtained for design purposes.

Table 1 - Theoretical-experimental values of mean-characteristic strength and modulus of elasticity

Tensile Strength			
	Experimental (MPa)		Theoretical (MPa)
	Weak axis	Strong axis	
Float Glass	33.58	32.64	40
Tempered Glass	121.7	169.27	120
Modulus of Elasticity			
	Experimental (MPa)		Theoretical (MPa)
	Weak axis	Strong axis	
Float Glass	57.15	62.1	70
Tempered Glass	55.74	62.58	70

3. HAND CALCULATIONS OF GLASS T-BEAMS

Dimensions of the T-Beam were selected as shown in Fig. 6. Simply supported T-Beam specimens were tested under 8-point loading both for beams with and without post-tensioning. The main reason for the 8-point loading test was to mimic a uniformly distributed loading case which was not studied in the literature and is a very common loading pattern. Furthermore, the post-tensioning tendon creates a reverse uplift force and bending moment which is very similar to the one created by a uniform loading, such that two effects cancel each other. The horizontal component of tendon force at each transfer point is small, beneficiary, and neglected for practical reasons. Maximum shear force, moment, and deflection of a simply supported T-beam with 8-point loads are calculated. Then, a stress check procedure was carried out for the float and tempered glass T-beam cases to calculate the maximum load that beams can bear.

Maximum load-carrying capacity (P_{max}) was calculated for float and tempered glass beams without post-tensioning by common formulas (Eq. (1)). The governing failure stress is considered to be the tensile strength; however, the compressive and shear strengths are also checked. The maximum deflection (δ_{max}) of the T-beam is calculated using the Moment Area Method (Eq. (2)) Calculation results of T-beam without post-tensioning are tabulated in Table 2.

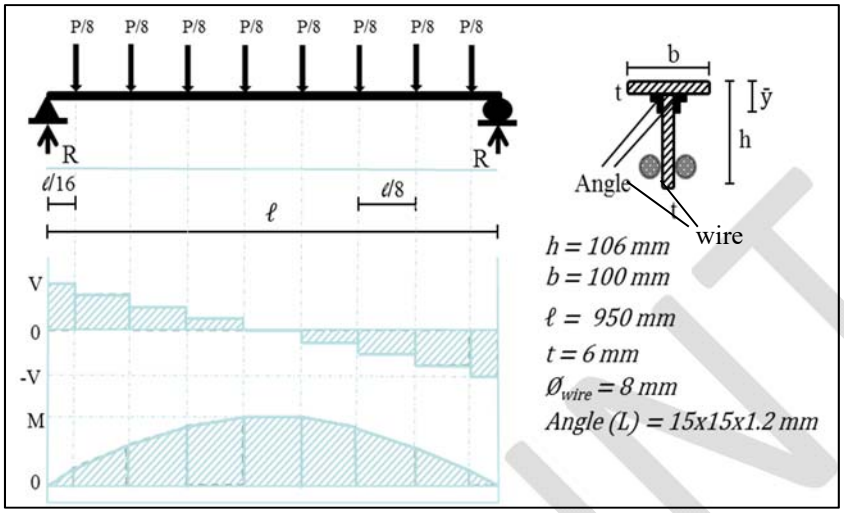

Fig. 6 - Cross-section, loading pattern, shear force, and moment diagrams of the T-beam

$$P_{max} = \frac{8 * \sigma_{bottom} * I_{beam}}{(h - \acute{y}_{beam}) * \ell} \quad (1)$$

$$\delta_{max} = \frac{658}{49152} \frac{P_{max} \ell^3}{E I_{beam}} \quad (2)$$

where I_{beam} stands for a moment of inertia, $\bar{y}_{beam}$ for neutral axis, and E for modulus of elasticity of the T-beam.

Table 2 - Calculation results of T-beam without post-tensioning

Parameters	Float Glass	Tempered Glass
P_{max} (kN)	4.86	25.19
δ_{max} (mm)	0.66	3.37
σ_{top}* (MPa)	11.94 < 400	61.94 < 400
σ_{bottom} (MPa)	32.64	169.27
$\tau_{neutral\ axis}$ (MPa)	5.34 < 36.4	25.83 < 92.3
$\tau_{glue\ line}$** (MPa)	4.50 < 36.4	21.79 < 92.3

*compression **at the web and flange connection

The post-tensioned glass T-beams shall be analyzed for transfer (short term) and final (long term) cases. The transfer case is when the beam is under its self-weight and post-tensioning

load; the final case is when the beam is subjected to all loads such as post-tensioning load, live load, self-weight, relaxation, etc. Shear force and moment diagrams due to post-tensioning are shown in Fig. 7.

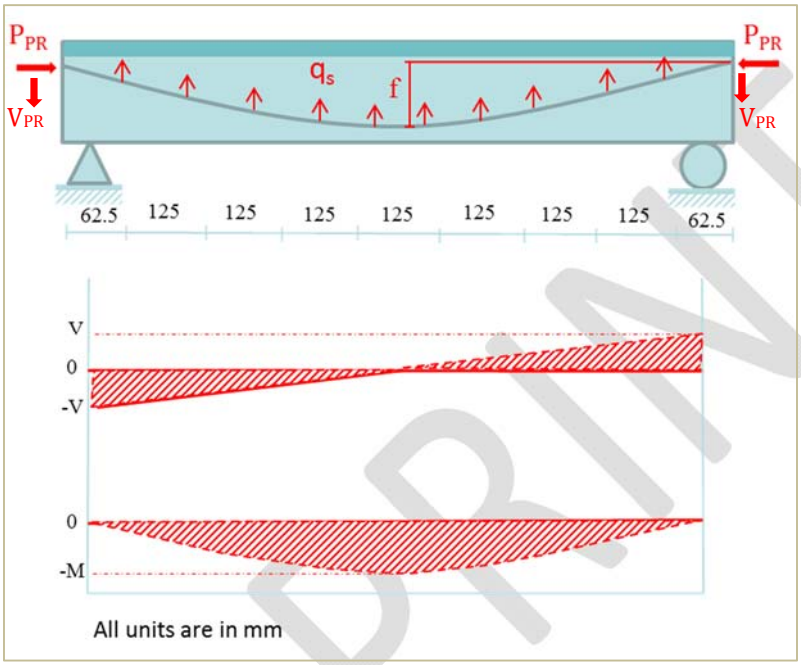

Fig. 7 - Shear force and moment diagrams due to post-tensioning

The post-tensioning force (P_{PR}) is calculated using Eq. (3) where f_u is the ultimate tensile strength and A is the cross-sectional area of tendon. The losses for post-tensioning were considered to be 15% to 25%. Moment due to post-tensioning (M_{PR}) is calculated by Eq. (4) and shear force (V_{PR}) by Eq. (5).

$$P_{PR} = (1\text{-Percentage of loss}) * (\text{Tensioning ratio}) * (f_u) * A_{tendon} \quad (3)$$

$$M_{PR} = P_{PR} * f = q_s * \frac{(\ell)^2}{8} = P * \ell/8 \quad => \quad q_s = \frac{8 * P_{PR} * f}{(\ell)^2} \quad (4)$$

$$V_{PR} = q_s * \frac{\ell}{2} \quad (5)$$

Stresses at the top and bottom ($\sigma_{top}, \sigma_{bottom}$) of the T-beams' mid-spans are calculated according to the equations for transfer and final cases (Eqs. (6), (7), (10), and (11)). Shear stress at neutral and glue points are calculated by Eqs. (8), (9), (12), and (13). In the equations below, $\Delta M_{transfer}$ is the moment at the mid-span of the T-beam under dead load and post-tensioned load, and ΔM_{final} is the moment at the mid-span of the T-beam under all loads

including post-tensioned load, $\Delta V_{transfer}$ is the shear force at the mid-span of the T-beam under dead load and post-tensioned load, and ΔV_{final} is the shear force at the mid-span of the T-beam under all loads including post-tensioned load,

Transfer (Short-term) Case

$$\sigma_{top} = \frac{-P_{PR}}{A_{beam}} - \frac{\Delta M_{transfer} * \bar{y}_{beam}}{I_{beam}} \quad (6)$$

$$\sigma_{bottom} = \frac{-P_{PR}}{A_{beam}} + \frac{\Delta M_{transfer} * (h-\bar{y}_{beam})}{I_{beam}} \quad (7)$$

$$\tau_{neutral\ axis} = \frac{\Delta V_{transfer} * Q_{neutral}}{I_{beam} * t} \quad (8)$$

$$\tau_{glue\ point} = \frac{\Delta V_{transfer} * Q_{glue\ point}}{I_{beam} * t} \quad (9)$$

Final (Long term) Case

$$\sigma_{top} = \frac{-P_{PR}}{A_{beam}} - \frac{\Delta M_{final} * \bar{y}_{beam}}{I_{beam}} \quad (10)$$

$$\sigma_{bottom} = \frac{-P_{PR}}{A_{beam}} + \frac{\Delta M_{final} * (h-\bar{y}_{beam})}{I_{beam}} \quad (11)$$

$$\tau_{neutral\ axis} = \frac{\Delta V_{final} * Q_{neutral}}{I_{beam} * t} \quad (12)$$

$$\tau_{glue\ point} = \frac{\Delta V_{final} * Q_{glue\ point}}{I_{beam} * t} \quad (13)$$

The maximum load ($P_{crack/ultimate}$) that the T-beam can sustain is calculated by Eq. (14). The maximum load for float glass is considered to be the cracking load while it is considered as an ultimate load for tempered glass.

$$P_{crack\ or\ ultimate} = \left(\frac{(\sigma_{bottom} + \frac{P_{PR}}{A_{beam}}) * I_{beam}}{(h-\bar{y}_{beam})} + M_{PR}\right) * \frac{8}{\ell} \quad (14)$$

All calculations for post-tensioned glass T-beams done tabulated in Table 3.

Compared with T-beam without post-tensioning, the maximum load that the same dimensioned T-beam can resist increased from 4.86 kN to 10.53 kN for float glass and from 25.19 kN to 39.97 kN for tempered glass. Theoretically, the tensile strength capacity increased substantially after the post-tensioning application.

Table 3 - Calculation results of post-tensioned T-beam

	Property	Float Glass	Tempered Glass
Transfer case	P_{PR} (kN)	8.26	21.54
	$\delta_{transfer}$ (mm)	0.62	1.60
	σ_{top} (MPa)	5.00	13.20
	σ_{bottom} (MPa)	-37.89	-99.38
Final case	$P_{crack/ult.}$ (kN)	10.53	39.97
	δ_{final} (mm)	0.81	3.754
	σ_{top} (MPa)	-20.68	-85.12
	σ_{bottom} (MPa)	32.30	169.47
	$\tau_{neutral\ axis}$ (MPa)	6.34	32.39
	$\tau_{glue\ line}$ (MPa)	5.34	27.32

4. NUMERICAL MODELING OF T-BEAMS

The finite element models (FEMs) of T-beams were modeled in structural software for analysis and design (SAP2000 v.20). Post-tensioned float and tempered glass T-beams were modeled as well as the models without post-tensioning. After defining the materials and sections, the T-beam was modeled as shown in Fig. 8.

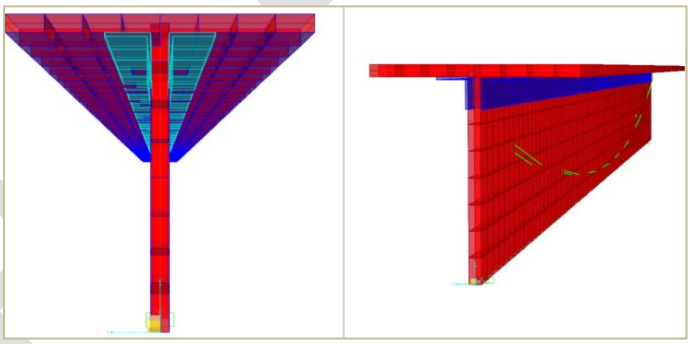

Fig. 8 - View of post-tensioned float glass T-beam FEM

In the T-beam structural model, glass, aluminum, and wire rope were defined. The aluminum was defined as AA6063-T6 from SAP2000 materials manual, while glass is defined as in Fig. 9.

The L-shaped aluminum angles were defined as 2x15x15x1.2 mm dimensioned double angle section with a back-to-back spacing of 6 mm (Fig. 10). The wire used in the specimen for post-tensioning is defined as a tendon as shown in Fig. 11.

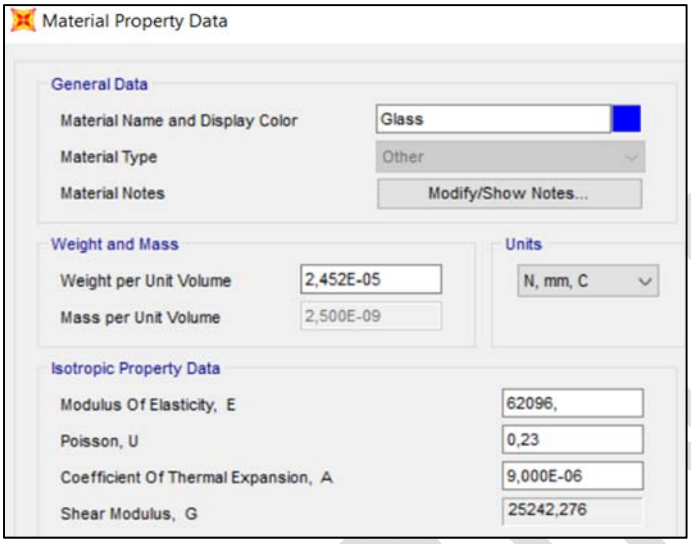

Fig. 9 - Material property data of glass

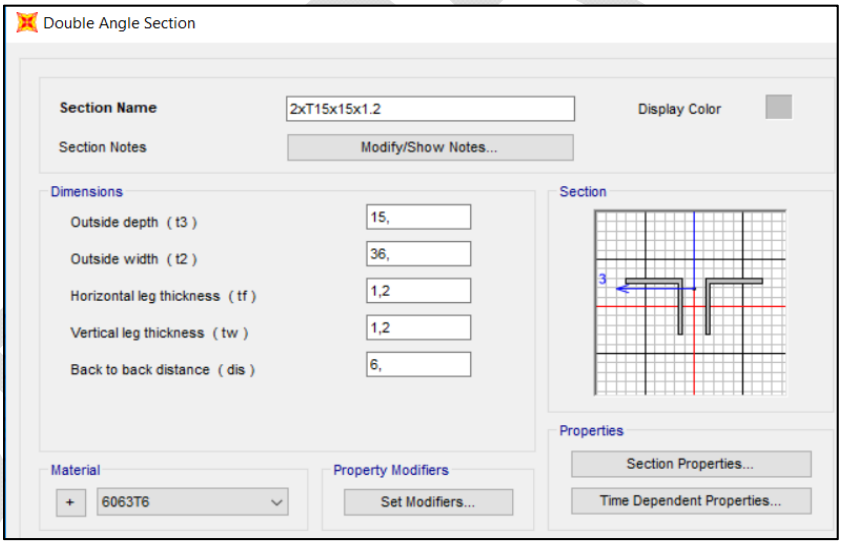

Fig. 10 - Aluminum double angle section definition

Then it was loaded to the maximum load found from calculations, the stress at the top and bottom of the mid-span of the beam was found both at transfer and final cases. The stress distribution at transfer case of post-tensioned float glass T-beam is displayed in Fig. 12, and at the final case in Fig. 13.

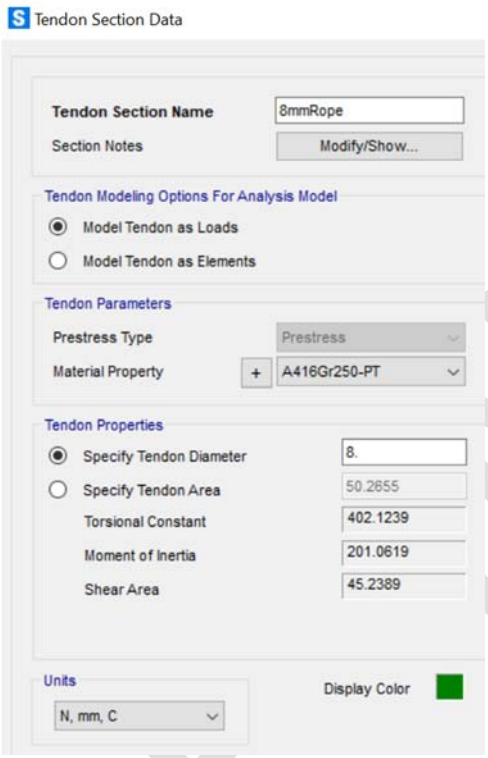

Fig. 11 - Tendon section data

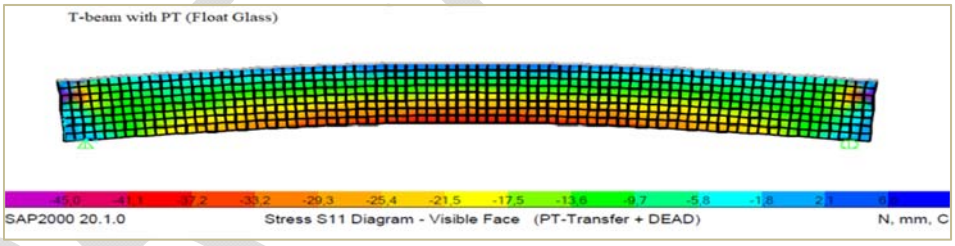

Fig. 12 - Stresses at transfer case of post-tensioned float glass T-beam

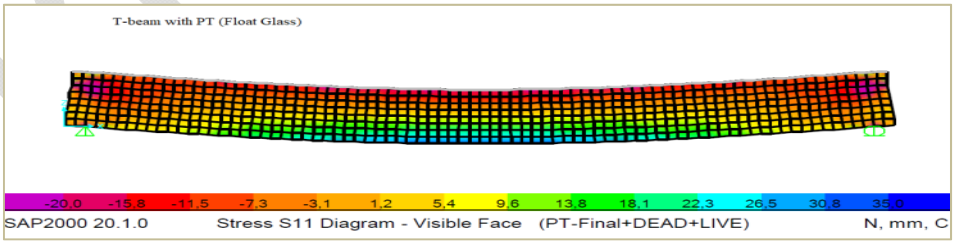

Fig. 13 - Stresses at the final case of post-tensioned float glass T-beam

FEM results of T-beams with post-tensioning at their mid-spans are tabulated in Table 4.

Table 4 - FEM results of T-beam with post-tensioning

Property	Float Glass		Tempered Glass	
	Transfer Case	Final Case	Transfer Case	Final Case
δ_{max} (mm)	0.70	0.82	1.84	3.92
$\sigma_{max,tensile}$ (MPa)	4.88	32.73	12.86	169.3
$\sigma_{max,compressive}$ (MPa)	-39.22	-23.82	-103.3	-95.89

Results taken from FEMs were close to hand calculations both for float and tempered glass types. The FEM results will be compared with hand calculations and experiment outputs and discussed in the following sections.

5. TESTS OF T-BEAMS

5.1. Test Setup and Components

T-beam specimens were prepared for the tests with and without post-tensioning. The web and flange of the T-Beam were 1000 mm in length, 100 mm in height, and 6 mm in thickness. The flange and web parts of the glass beam were bonded with two aluminum L profiles in 15x15x1.2 mm dimensions with the help of polyurethane-based adhesive as a bonding material. Aluminum alloy AA6063-T6 type is used. The parabolic shape of the wire rope and coordinates of the brass connection points are shown in Fig. 14. All the units given in the figure are in millimeters.

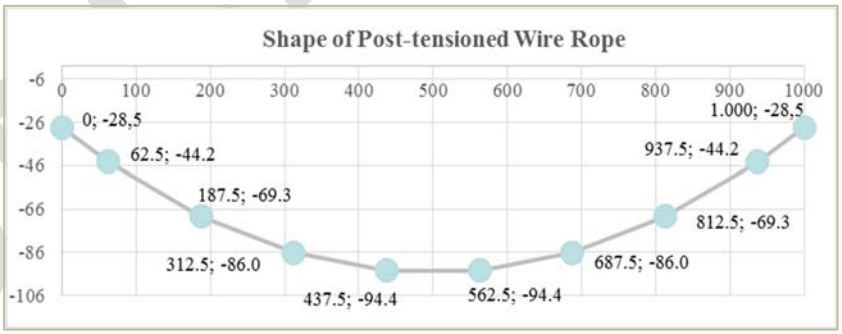

Fig. 14 - Geometry and coordinates of post-tensioned wire rope connectors

The set-up of a T-beam sample without post-tensioning is displayed in Fig. 15a and the set-up of post-tensioned T-beam in Fig. 15b.

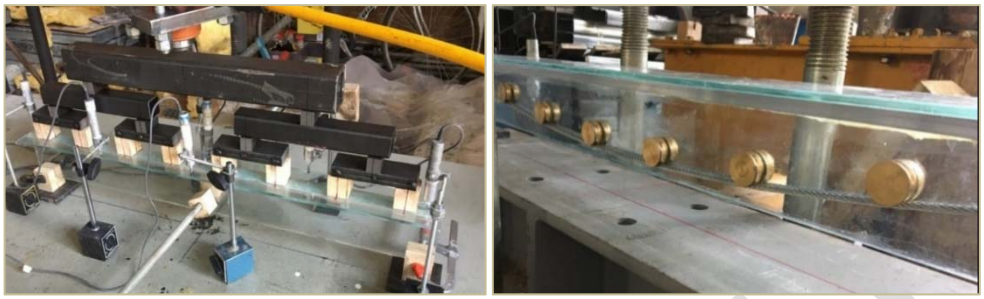

a) b)

Fig. 15 - Test set-up of T-beam (a) without post-tensioning and (b) with post-tensioning

5.2. Conducting the Tests and Obtaining the Results

Three specimens of each type (float and tempered) of T-beams with and without post-tensioning tests were conducted. The specimens were loaded until their fracture point. The float glass without post-tensioning fractured at the constant moment zone due to tensile stress. The crack started at the constant moment zone of the tensile area and fragmented upwards to the compression zone (Fig. 16).

Fig. 16 - Float glass T-beam exposed to its cracking load

Fig. 17 - Tempered glass T-beam exposed to its ultimate loading

Tempered glass T-beam fractured into small pieces at its ultimate load in the maximum moment zone without any ductility as shown in Fig. 17.

The load-displacement graphs of float and tempered glass T-beam specimens are given in Fig 18. Rapid unloading at about 10 kN and 15 kN loads indicated some energy dissipating mechanisms, which may be related to the hydraulic loading jack's damping properties. However, no residual deformations were observed as all tests returned to their original starting points.

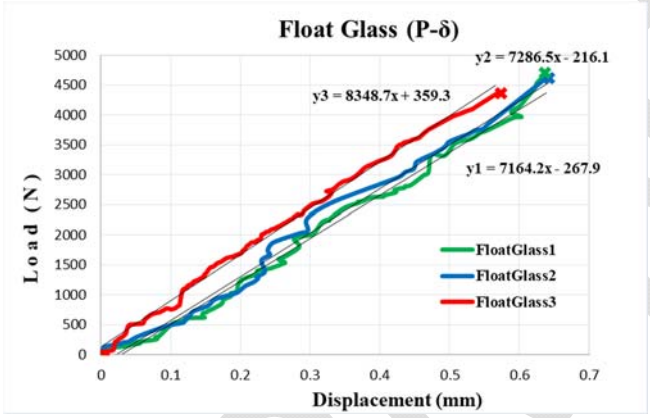

(a)

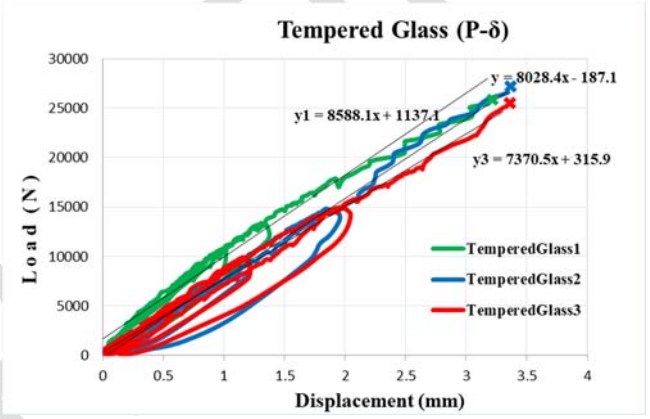

(b)

Fig. 18 - Load-displacement graph of (a) float and (b) tempered glass T-beam without post-tensioning

Although promising results were obtained from the tests compared with hand calculations and FEMs, the modulus of elasticity and characteristic strength of the T-beam without post-tensioning are also calculated as it was done for material tests. The aim was to confirm whether the T-beam concept was proper with the bonding material and aluminum L-shaped angle. The results of the modulus of elasticity and characteristic strength calculations are given in Table 5.

Table 5 - Calculation results of characteristic modulus of elasticity and strength for glass T-beam samples

	Characteristic Tensile Strength (MPa)	Characteristic Modulus of Elasticity (GPa)
Float Glass	29.34	52.21
Tempered Glass	160.04	61.23

As it is seen, the characteristic strength and modulus of elasticity results obtained for the T-beam were almost the same results in the material tests, so the glue material used and the T-beam concept were accepted.

The T-beams for post-tensioning tests were prepared in the same way as the T-beam without post-tensioning. The tests conducted for T-beams with post-tensioning were the most crucial and difficult part of the study since the wire rope slipping problem had to be overcome. This problem was overcome with grips used at the supports which are used to grasp wires tightly with no movement. After the setup was prepared, the wire rope was tensioned to 8.25 kN for float glass and to 21.58 kN for tempered glass. These post-tensioning forces were determined by following the standard procedure of concrete beams except for shrinkage losses. The relaxation, slippage, and creep losses were considered and transfer stresses (tension at the top) and design loads (tension at the bottom) were considered. Web shear, support bearing, flange-web shear transfer, flange, and web buckling checks were made.

Starting loading, the first crack was observed at the maximum moment region in the tests of float glass with post-tensioning. As the loading progressed, more cracks were observed propagating towards the supports of the beam and from the bottom (tension) to the top (compression) zone (Fig. 19).

Deflection-controlled loading test results for the post-tensioned float glass T-beam are given in Fig. 20. The graph shows how the mid-span of the beam deflects with post-tensioning load and vertical loading. The upward direction was assumed a positive deflection and the downward as a negative deflection.

The float glass T-beam deflected 0.62 mm upward at its mid-span when post-tensioning of 8.25 kN is applied (Point 1 in Fig. 20). Then, the beam was loaded at 8 points in a pattern close to uniform loading and cracked at 10.86 kN corresponding to 0.749 mm downward deflection at the mid-span (Point 2 in Fig. 20). The cracks first appeared around the maximum bending moment zone at the mid-span and then spread out towards the supports while the beam was continued to be loaded (Between points 2 and 3 in Fig. 20). The fluctuations occurred as a result of progressing cracks.

The beam was unloaded at 15.72 kN load which corresponds to 12.5 mm deflection at its mid-span, where cracks were too large to proceed with the test (Point 3 in Fig. 20). The tests for the second and the third samples of post-tensioned float glass T-beams were conducted the same way and the results were all close to each other.

The tempered glass T-beam with post-tensioning fractured into small pieces at its cracked & ultimate load condition as shown in Fig. 21.

Fig. 19 - Float glass T-beam with post-tensioning after the fracture.

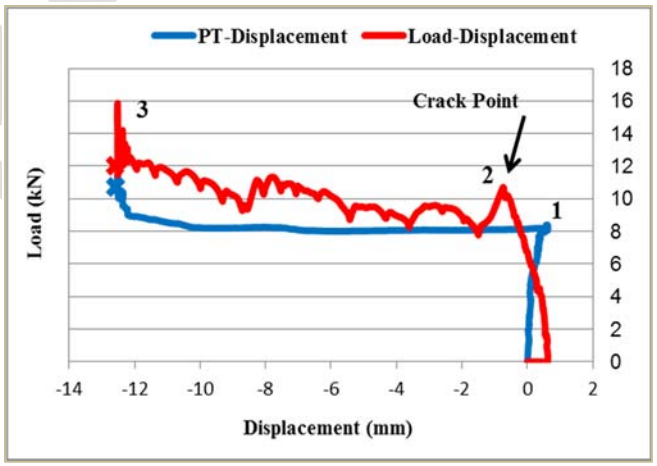

Fig. 20 - Load-displacement graph of post-tensioned float glass T-beam

Fig. 21 - Post-tensioned tempered glass T-beam after fracture.

The tempered glass T-beam had been post-tensioned to 21.54 kN. The sample deflected 1.66 mm in an upward direction upon post-tensioning (Point 1 in Fig. 22). Then, the beam was loaded at 8 points and started to deflect downward. The first sample cracked at 37.98 kN corresponding to 4.26 mm downward deflection at its mid-span. The first crack also marked the ultimate load capacity of the beam since tempered glass breaks in an explosive manner separating into small pieces of glass (Point 2 in Fig. 22).

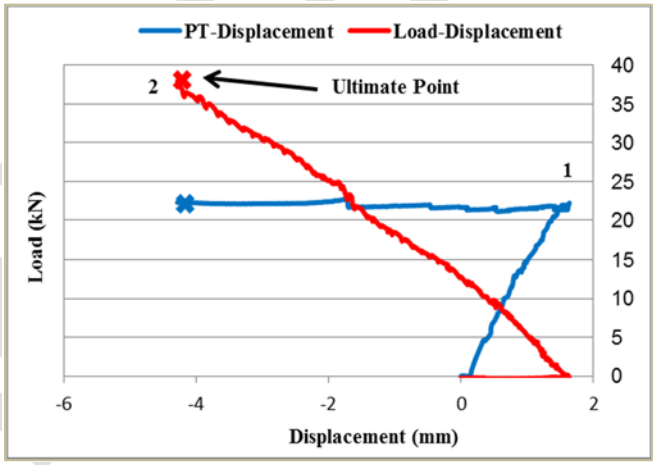

Fig. 22 - Load-displacement graph of post-tensioned tempered glass T-beam

The loading tests were repeated three times on similar samples and the average test results of T-beam samples are summarized below (Table 6).

After the tests, it was seen that T-beams without post-tensioning had a brittle failure. The tempered glass beam failed at 25.69 kN, which is 5.39 times higher than the float glass beam failure at 4.76 kN. Tempered glass T-beam with post-tensioning again had a brittle failure

but at 1.55 times higher load (39.79 kN) compared with the same tempered glass T-beam without post-tensioning. The capacity increase of the maximum load that T-beams with post-tensioning can resist depends on the post-tensioning design such as the tensioning ratio, the quantity of the wire rope, etc. However, a more preferable result was obtained from post-tensioned float glass which had a ductile failure. The crack load was 11.15 kN, which is 2.34 times higher than the same beam without post-tensioning. Moreover, the ultimate load was recorded as 19.28 kN, which is 4 times higher than the load float glass T-beam without post-tensioning can sustain. The comparisons between different types of the same dimensioned T-beams according to the test results are displayed in a column chart in Fig. 23.

Table 6 - Summary of T-beam test results

	T-beam without PT		T-beam with PT	
	Float Glass	Tempered Glass	Float Glass	Tempered Glass
Pcrack/ultimate (kN)	4.76	25.69	11.14	39.79
δmax (mm)	0.63	3.28	0.75	4.05

The capacities are accepted to be the cracking point, even though the post-tensioned float glass T-beam had post-tensioning ductile behavior. It can be concluded that the most preferable result was obtained from post-tensioned float glass, which had a ductile failure and a good post-fracture performance. The same amount of tempered glass may provide up to 4 times the strength; nevertheless, a sudden brittle failure may not be acceptable.

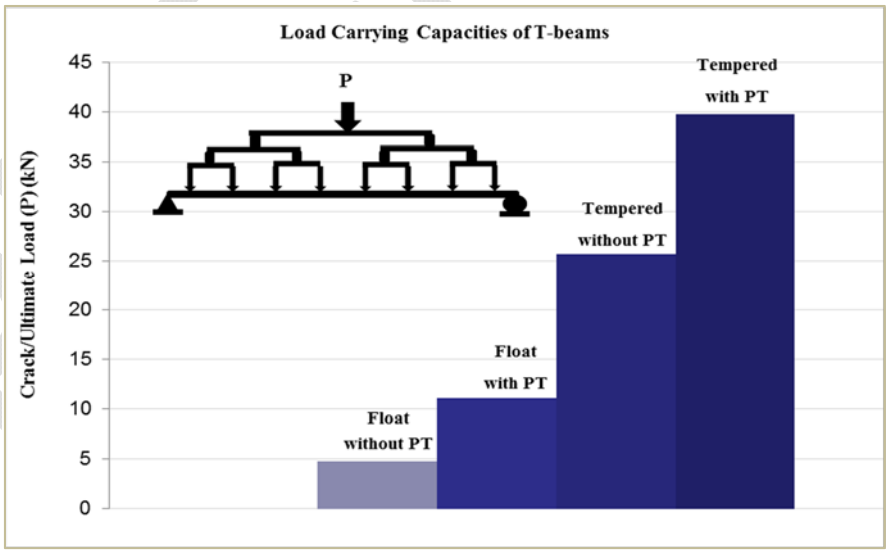

Fig. 23 - Load-carrying capacities of the same dimensioned T-beams

The results for T-beam of finite element models (FEMs), hand calculations, and tests were compared with load-deflection behavior and tabulated in Table 7 for T-beams without post-tensioning and in Table 8 for post-tensioned T-beams.

Table 7 - Summary of the results for T-beam without post-tensioning

	Float Glass		Tempered Glass	
	P_{crack} (kN)	δ_{max} (mm)	$P_{crack/ultimate}$ (kN)	δ_{max} (mm)
Hand Calc.	4.86	0.66	25.19	3.37
FEM	4.86	0.70	25.19	3.64
Test	4.76	0.63	25.69	3.28

Table 8 - Summary of the results for T-beam with post-tensioning

	Float Glass		Tempered Glass	
	P_{crack} (kN)	δ_{max} (mm)	$P_{crack/ultimate}$ (kN)	δ_{max} (mm)
Hand Calc.	10.53	0.81	39.97	3.75
FEM	10.53	0.82	39.97	3.92
Test	11.14	0.75	39.79	4.05

Comparison of hand calculations and FEM analyses with the test results showed a good correlation within the range of about ±3%. These results can be deemed as in good agreement, considering that the glass test results had a scatter of about ±4%. It can be concluded that both hand calculations and FEMs are valid for the design of post-tensioned glass T-beams.

6. CONCLUSION AND FUTURE WORK

The chosen problem is to investigate the feasibility of using post-tensioning to improve the structural performance of glass beams, specifically T-shaped beams. The use of glass as an architecturally appealing and structurally high-strength material (float glass tension capacity 40 MPa compression capacity 400 MPa and tempered glass tension capacity 120 MPa compression capacity 400-800 MPa) for load-carrying members is studied. The study includes numerical and experimental work on T-shaped glass beams considering post-tensioning. A minimalistic geometric approach was taken with the T-shape as the floor formed the top flange. One of the best outcomes of this study is that float glass post-cracking deflection can be drastically increased in a ductile manner while about a 55% increase in strength is achieved. This means that glass may be used as a beam in the construction field.

Comparison of the hand calculations, FEM analyses, and test results gave close values; therefore, analyses are close to the experimental results showing confidence for design.

Although the capacity of tensile strength increased in tempered glass T-beam, it still fractured and collapsed suddenly at its ultimate strength as expected. However, the superior post-cracking performance was achieved for post-tensioned float glass as an additional safety property even though glass is a brittle material.

Studies for the behavior of laminated or heat-strengthened glass with samples being tested under combined or more complex loading scenarios may be studied as future work. Also, glass being a visco-elastic material having some liquid-like properties, post-tensioned glass beams may be better checked for post-tensioning force losses at certain time intervals. Furthermore, exploring practical methods for fabricating, installing, and maintaining post-tensioned glass beams in real-world applications and analyzing the life cycle assessment of post-tensioned glass T-beams to understand their environmental impact compared to traditional materials contributes to the usage of glass as a viable and sustainable option for modern architecture.

References

[1] Super safe CE certified 13.52 mm laminated glass panels for padel tennis court (2021, November) https://www.szdragonglass.com/13-52-laminated-glass-panels-for-padel-court/

[2] BS EN 572-1 (2004), Glass in Building - Basic soda lime silicate glass products Part 1: Definitions and general physical and mechanical properties, European Committee for Standardization.

[3] EN 572-2 (2004), Glass in Building - Basic Soda Lime Silicate Glass Products - Part 2: Float Glass, European Committee for Standardization.

[4] Cupać, J., Louter, C., & Nussbaumer, A. (2021). Flexural behaviour of post-tensioned glass beams: Experimental and analytical study of three beam typologies. Composite Structures, 255, 112971.

[5] Belis, J., Van Impe, R., Lagae, G. and Vanlaere, W. (2003), "Enhancement of the buckling strength of glass beams by means of lateral restraints.", Structural Engineering and Mechanics, 15(5), 495-511. https://doi.org/10.12989/sem.2003.15.5.495.

[6] Louter, C., Heusden, J. Veer, F., Vambersky, J., Boer, H., Versteegen, J. (2006), "Post-tensioned glass beams.", https://www.researchgate.net/publication/241016445_Post-Tensioned_Glass_Beams

[7] Belis, J., Louter, C., Verfaille, K., Van Impe, R., and Callewaert, D. (2006), "The effect of post-tensioning on the buckling behaviour of a glass T-beam.", Proceedings of International Symposium on the Application of Architectural Glass, (129-136).

[8] Louter, C. (2011), "Fragile yet Ductile, Structural Aspects of Reinforced Glass Beams". Ph.D. Dissertation, Technische Universiteit, Delft.

[9] Louter, C., Cupac, J., and Lebet, J. P. (2014), "Exploratory experimental investigations on post-tensioned structural glass beams.", Journal of Façade Design and Engineering, 2(1-2), 3-18. DOI: 10.3233/FDE-130012

[10] Engelmann, M., Weller, B. (2016), "Post-tensioned Glass Beams for a 9 m Spannglass Bridge.", Structural Engineering International, 26(2), 103-113. DOI: 10.2749/101686616X14555428759000

[11] Cupać, J., Louter, C., & Nussbaumer, A. (2021). Post-tensioning of glass beams: Analytical determination of the allowable pre-load. Glass Structures & Engineering, 6(2), 233-248.

[12] Weller, B. and Engelmann, M. (2014), "Deformation of Span-glass beams during post-tensioning", Proceedings of Challenging Glass 4 & Cost Action TU0905 Final Conference, London, United Kingdom. https://www.researchgate.net/publication/290179946_Deformation_of_Spannglass_beams_during_post-tensioning

[13] Jordão, S., Pinho, M., Martins, J.P., Santiago, A., and Neves, L.C. (2014), "Behaviour of laminated glass beams reinforced with pre-stressed cables.", Steel Constr., 7(3), 204–207. https://doi.org/10.1002/stco.201410027

[14] Bedon, C. and Louter, C. (2016), "Finite-element analysis of post-tensioned SG-laminated glass beams with mechanically anchored tendons.", Glass Struct Eng, 1, 39–59. https://doi.org/10.1007/s40940-016-0020-7.

[15] Cupać, J., Martens, K., Nussbaumer, A. et al. (2017), "Experimental investigation of multi-span post-tensioned glass beams.", Glass Struct Eng, 2, 3–15. https://doi.org/10.1007/s40940-017-0038-5.

[16] Ugural AC, Fenster SK. Advanced Strength and Applied Elasticity. 4th ed. New Jersey: Prentice Hall; 2003, p. 160-161.